

BBAMEM 74743

## Interaction of Triton X-100 and octyl glucoside with liposomal membranes at sublytic and lytic concentrations. Spectroscopic studies

J. Lasch<sup>1</sup>, J. Hoffmann<sup>1</sup>, W.G. Omelyanenko<sup>2</sup>, A.A. Klibanov<sup>2</sup>, V.P. Torchilin<sup>2</sup>,  
H. Binder<sup>3</sup> and K. Gawrisch<sup>3</sup>

<sup>1</sup> Institut für Biochemie, Bereich Medizin, Martin-Luther-Universität, Halle / Saale (G.D.R.), <sup>2</sup> All-Union Research Center of Cardiology, Medical Academy of Science, Moscow (U.S.S.R.) and <sup>3</sup> Sektion Physik, Bereich Molekülphysik, Karl-Marx-Universität, Leipzig (G.D.R.)

(Received 12 June 1989)

(Revised manuscript received 1 October 1989)

**Key words:** Liposome–detergent interaction; Detergent, neutral; Lipid–detergent ratio; Bilayer solubilization

The molecular mechanism of the solubilisation of phospholipid bilayers by nonionic detergents was studied by turbidity changes, carboxyfluorescein fluorescence dequenching, steady-state and time-resolved fluorescence anisotropy of DPH, lifetime measurements, ANS binding and <sup>31</sup>P-NMR. Particular attention has been paid to the effective detergent-to-lipid ratio in the lipid phase. The disturbance of the bilayer arrangement varies considerably for various detergents depending on the hydrophilic and lipophilic parts of the molecule. Small amounts of detergents with low CMC (e.g. Triton X-100) can even induce an optimisation of packing of the lipid molecules.

### Introduction

During recent years much attention has been paid to the interaction of detergents with natural and artificial phospholipid membranes [1–5].

Nonionic detergents are widely used as molecular tools in membranology. Their applications include disintegration of biomembranes to mixed micelles [6], reconstitution of membrane protein and lipid to functional supramolecular structures (vesicles in most cases) [7,8] and preparation of liposomes of homogeneous and controlled size [9,10].

It is generally accepted now, that, as originally proposed by Helenius and Simons [1], the conversion of phospholipid bilayers into mixed micelles with increasing amounts of detergent occurs in three steps: in stage I there exists an equilibrium distribution of the detergent between the lipid and water phase; in stage II mixed bilayers coexist with mixed micelles, the former

are transformed progressively into mixed micelles as the detergent concentration increases until all of the bilayers have disappeared in stage III. In this stage the micelles grow gradually richer in detergent with a concomitant decrease in particle size. In a large number of studies this simple scheme has been corroborated, extended and quantitatively characterised [2–4,11–13]. Little detailed information, however, exists about stage II which is the most interesting one from a mechanistical point of view and the most difficult to approach experimentally.

All physical parameters used to quantitatively characterise the interaction between lipid bilayers and detergents critically depend on the amount of detergent partitioned into the lipid phase at a given total detergent to lipid ratio. It must be emphasised, however, that the correct variable is the detergent-to-lipid ratio in the lipid phase, the effective ratio, which can be calculated if the partition coefficient is known. Its importance for the understanding and quantitative description of membrane solubilisation has been pointed out in a recent paper by Lichtenberg [3]. Two problems remain, however, largely unsolved. First, using the bubble pressure technique [5], we found (unpublished results) that partition coefficients of some detergents (e.g., octyl glucoside, sulfobetaines, diisooctyl sulfosuccinate), which are constant in the range where the total detergent concentration is much lower than the lipid concentration,

Abbreviations: ANS<sup>-</sup>, 8-aminonaphthalene 1-sulphonate; CF, carboxyfluorescein; CMC, critical micellar concentration; EPC, egg phosphatidylcholine; OG, octyl glucoside.

Correspondence: J. Lasch, Institut für Biochemie, Bereich Medizin, Martin-Luther-Universität, PF 184, Halle/Saale, DDR-4010, G.D.R.

increase linearly when the detergent approaches and exceeds the lipid concentration even if its total concentration is as low as one-tenth of the CMC. Thus, partition coefficients measured at low detergent concentrations are not necessarily the same as those at the onset of stage II of solubilisation. Concentration-dependent partition coefficients have been reported for other compounds too, e.g., phenol and anaesthetics [14,15].

On the other hand, there might be no ideal mixing of detergent and lipid resulting in lipid-associated detergent with a chemical potential varying with its location, limited to a narrow space not much different from a binding site. Is binding or partitioning then the better description?

In this work, we have studied the interaction of octyl glucoside and Triton X-100 with small unilamellar liposomes by a variety of techniques (turbidity, carboxyfluorescein fluorescence dequenching, steady-state and time-resolved fluorescence anisotropy of DPH, lifetime measurements, ANS binding and  $^{31}\text{P}$ -NMR) with the aim to gain insight into the molecular mechanism of solubilisation in stage II. Particular attention has been paid to the effective detergent-to-lipid ratio within the lipid membrane.

## Materials and Methods

Egg yolk phosphatidylcholine (Kharkov, U.S.S.R.) and dipalmitoylphosphatidylcholine (Calbiochem, U.S.A.), dissolved in chloroform or ethanol, were flushed with nitrogen or argon, dispersed in buffer (Tris 50 mM, pH 7.4) and sonicated to a clear suspension under cooling with a tip sonifier (Branson Sonifier B-12 or Lab-Line Ultratip). Gel chromatography on Sepharose CL-4B revealed only negligible amounts of oligolamellar vesicles. Reverse phase evaporation vesicles were prepared as described in Ref. 15.

Lipid concentrations were assayed colorimetrically essentially as described by Stewart [16]. Calibration curves, run with DPPC, were linear in the range of 1–30  $\mu\text{g}$ . Triton X-100, ANS, DPH and octyl glucoside were purchased from Serva (Heidelberg, F.R.G.).

Turbidities were recorded on the Shimadzu UV 300 spectrophotometer (Kyoto, Japan) at 420 nm or Eppendorf Photometer M 1100 (Hamburg, F.R.G.) at 334 nm.

Permeation of the trapped fluorescent marker carboxyfluorescein through liposomal bilayers was monitored by the fluorescence increase accompanying the dilution of self-quenched CF into the surrounding medium [17]. Release kinetics were followed with the Perkin Elmer MPF 44 (excitation, 492 nm; emission, 516 nm; temperature, 25°C). CF leakage obeyed first-order kinetics. Velocity constants, according to the kinetic model  $y = y_0(1 - \exp(-kt))$ , were evaluated from the slopes of the linear plots  $\ln((\text{SU}_{\text{max}} -$

$\text{SU}_0)/(\text{SU}_{\text{max}} - \text{SU}_t) = kt$ , where  $\text{SU}_0$ ,  $\text{SU}_t$  and  $\text{SU}_{\text{max}}$  stand for scale units at time zero, time  $t$  and after total solubilisation by detergent, respectively. Permeability coefficients were obtained from the relation:

$$P = k \cdot (\text{internal volume/vesicle} : \text{membrane area/vesicle})$$

Total trapped volume was determined from the absorbance of liposomally entrapped potassium dichromate according to

$$V_{\text{tr}} = A_2 V_1 / A_1$$

$V_1$ , total sample volume,  $A_1$ , absorbance of starting solution (200 mM  $\text{K}_2\text{Cr}_2\text{O}_7$ ) and  $A_2$ , absorbance after lysis of dichromate-loaded liposomes (external dichromate was previously removed by gel filtration on Sephadex G-50). The trapped volume per mole of phospholipid was used as a measure of the apparent vesicle diameter by simple geometric calculations similar to those in Table I of Mimms et al. [18].

Phase transitions were followed photometrically taking advantage of the change in Mie scattering during chain melting [19]. Melting curves were recorded with the Beckman DU-8B spectrophotometer (Irvine, U.S.A.) equipped with a programmable temperature control unit. DPPC liposomes were scanned from 25°C up to 55°C and thereafter in the reverse direction in steps of 0.5 or 1.0°C with intervals of 1 min to allow for thermal equilibration. Melting curves, recorded at increasing and decreasing temperatures, were symmetrical and reproducible.  $T_m$  values were assigned by projecting the midpoints of the scattering absorption transitions on the temperature axis.

Steady-state fluorescence and anisotropy of DPH and ANS were obtained with the Aminco SPF-500 fluorimeter (Silver Spring, U.S.A.) in ratio mode, using Polaroid sheet polarisers for measurements of polarised fluorescence. The steady-state anisotropy of DPH incorporated into liposomes was calculated according to

$$r = (I_{\text{VV}} - G \cdot I_{\text{VH}}) / (I_{\text{VV}} + 2G \cdot I_{\text{VH}})$$

$I_{\text{VV}}$  vertical and  $I_{\text{VH}}$  horizontal component of emission when excited with vertically polarised light. The correction factor for differences in the transmission of vertically and horizontally polarised light through the optical system was  $G = I_{\text{VH}}/I_{\text{HH}} = 0.87$ . Samples were sufficiently diluted so that contributions of scattered light became negligible (<1%). Anisotropy decay data of DPH were collected with a modified LIF 200 nitrogen laser pulse fluorimeter (ZWG, Berlin). Excitation light (337.1 nm) was passed through a Glan Thompson polarizer. Emitted light was collected at 90° through sheet polarizers. The instrument response function,  $g(t)$ , had a full width at half-maximum of about 3 ns. The time base was 0.22 ns per channel.

Analysis of time-resolved fluorescence anisotropy. The total fluorescence intensity  $I_T(t)$ , the difference intensity  $I_D(t)$  and the anisotropy  $r(t)$  were obtained from the observed intensities  $I_{VV}(t)$  and  $I_{VH}(t)$  according to

$$I_T(t) = I_{VV}(t) + 2G \cdot I_{VH}(t)$$

$$I_D(t) = I_{VV}(t) - I \cdot G_{VH}(t)$$

$$r(t) = I_D(t)/I_T(t)$$

The correction factor  $G$  is given by

$$G = [(1-r)/(1+2r)] \cdot (\sum I_{VH}(t)/\sum I_{VV}(t))$$

where  $r$  denotes the steady-state anisotropy of the sample determined as described above and  $\sum$  refers to the summation of the respective intensity data over time [20].

The fluorescence and anisotropy decays were analysed by assuming exponential impulse responses of the form:

$$i_T(t) = a_1 \exp(-t/\tau_1) + a_2 \exp(-t/\tau_2) \quad (1)$$

$$r(t) = (r_0 - r_\infty) \exp(-t/\phi) + r_\infty \quad (2)$$

The amplitudes  $a_{1,2}$ , fluorescence lifetimes  $\tau_{1,2}$ , limiting anisotropy  $r_\infty$ , anisotropy at time zero  $r_0$  and the characteristic time  $\phi$  of relaxation into the anisotropic equilibrium distribution of the probe were determined by nonlinear least-squares regression. To this end, the convolution products  $g(t) \otimes i_T(t)$  and  $g(t) \otimes [i_T(t) \cdot r(t)]$  were fitted to the  $I_T(t)$  and  $I_D(t)$  data, respectively. We chose to treat  $r_0$  as a free parameter in the fitting procedure. Curve fitting yielded values in the range of 0.30–0.39 which is somewhat lower than the fundamental anisotropy in isotropic rigid media. This was explained earlier by others [21] as being due to depolarising effects in vesicle systems. The mean excited state lifetime of DPH was calculated from

$$\langle \tau \rangle = \sum a_i \tau_i^2 / \sum a_i \tau_i \quad i=1, 2$$

The parameters  $r_0$ ,  $r_\infty$  and  $\phi$  are interpreted within the framework of the 'wobbling-in-cone model' [22]. The orientational order parameter  $S_{DPH}$  [23,24] and the wobbling diffusion constant  $D_w$  [25] of the fluorescent probe were calculated from the following equations:

$$r_\infty/r_0 = x^2(1+x)^2/4 = S_{DPH}^2 \quad (3)$$

$$D_w = r_0/(\phi(r_0 - r_\infty)) \cdot f(x) \quad (4)$$

In Kinosita's wobbling-in-cone model of rotational diffusion of rod-shaped fluorophores in lipid membranes  $x = \cos \theta$ , where  $\theta$  is half the opening angle of the cone

within which the probe wobbles\*. We treat here  $x$  just as an unknown, which can be calculated from  $r_\infty/r_0$  according to Eqn. 3 and inserted into Eqn. 4 in order to compute  $D_w$  (for the exact rather complex expression of  $f(x)$ , see Eqn. 24 in Ref. 25). While the quantities  $S_{DPH}^2$  and  $r_\infty$  report about the degree of confinement of orientation of the fluorescent marker imposed by the environment of the lipid bilayer,  $D_w$  provides us with a measure of the average speed with which the molecule wobbles within the confined angle.

Within certain limits the steady-state anisotropy  $r$ , because of the empirical relation  $r_\infty = (4/3)r - 0.1$ , provided the inequality  $0.13 < r < 0.28$  [23,24] holds, also yields information about structural order.

Fluorescence lifetime measurements of  $ANS^-$  were performed by the single-photon counting technique. The optical part of the instrument was from Applied Photophysics Ltd. (London), the time-to-amplitude converter from Ortec (Tennessee, U.S.A.) and the multi-channel pulse height analyser, Ino Tech 5400, from the Norland Inc. (U.S.A.). Data were collected, deconvoluted and fitted by a Labtam 3000 computer (Australia). The fluorescence decay was analysed by multi-exponential components and the goodness of fit assessed by  $\chi^2$  and plots of normalised residuals. The samples were excited with 4 ns pulses at a repetition rate of 50 kHz. The maximal number of counts accumulated per channel was set to 10000.

The binding of the fluorescent probe  $ANS^-$  was studied to gain information about the influence of increasing detergent concentrations on the structure and mobility in the polar headgroup region [26]. Detergents were added to dilute liposomes (final lipid concentration: 0.1 mM) in such amounts that all three stages of solubilisation were obtained. These samples were titrated with  $ANS^-$  dissolved in buffer (3 mM) and the fluorescence intensity and lifetime measured at 475 nm (excitation: 360 nm). The medium contained 0.1 M NaCl in order to reduce the influence of electrostatic interactions at the bilayer surface on the binding constant\*\*.

The observed fluorescence signal of sufficiently diluted  $ANS^-$  liposome mixtures is given by

$$I_{475} = g \cdot \epsilon \cdot (Q_b \cdot (ANS^-)_b + Q_f \cdot (ANS^-)_f) \quad (5)$$

provided there are no inner filter effects and no Förster-type energy transfer. The symbols  $g$ ,  $\epsilon$ ,  $Q_{b,f}$  represent, respectively, an instrumental proportionality constant, the absorption coefficient at the excitation

\*  $\theta$  is defined as the angle at which a rod-shaped membrane probe encounters an infinite energy barrier.

\*\* It is well known [26] that the binding constant is a function of the surface potential of the membrane  $\psi_0$  according to  $K = K_0 \cdot \exp(e\psi_0/kT)$  where  $K_0$  is the binding constant in the absence of a surface potential.

wavelength and the quantum yields of the bound and free probe. The quantum yield of free  $\text{ANS}^-$  in the aqueous phase can be neglected ( $Q = 0.004$  [27]) yielding:

$$I_{475} = g' \cdot Q_b \cdot (\text{ANS}^-)_b \quad (6)$$

where  $(\text{ANS}^-)_b$  is the concentration of bound  $\text{ANS}^-$ . And, as the quantum yield is proportional to the lifetime

$$I_{475} = g'' \cdot \tau \cdot (\text{ANS}^-)_b \quad (7)$$

In order to evaluate  $g''$ , fluorescence and lifetime of  $\text{ANS}^-$  were measured in ethanol in which the fluorescent probe has a nearly identical emission spectrum as in lipids so that we can put

$$g'' = I_{\text{ethanol}} / (\tau_{\text{ethanol}} \cdot (\text{ANS}^-)_{\text{ethanol}})$$

A 0.06 mM solution yielded

$$g'' = 4.1 / (8.12 \cdot 6 \cdot 10^{-5}) = 8.41 \text{ (ns}^{-1} \cdot \text{mM}^{-1}\text{)}$$

$(\text{ANS}^-)_b$  in the liposomal system was then obtained from values of  $I_{475}$  and lifetime, measured at various total amounts of  $\text{ANS}^-$  added, according to Eqn. 7.

The free  $\text{ANS}^-$  concentration  $(\text{ANS}^-)_f$  is obtainable from the conservation equation  $(\text{ANS}^-)_{\text{total}} = (\text{ANS}^-)_b + (\text{ANS}^-)_f$ . The binding capacity  $B$  and dissociation constant  $K_D$  are then found by fitting  $(\text{ANS}^-)_b$  and  $(\text{ANS}^-)_f$  to the Langmuir-type binding isotherm

$$(\text{ANS}^-)_b = B \cdot (\text{ANS}^-)_f / (K_D + (\text{ANS}^-)_f)$$

the dissociation constant being defined by

$$K_D = (\text{ANS}^-)_f \cdot (B - (\text{ANS}^-)_b) / (\text{ANS}^-)_b$$

Assuming that lipid as well as lipid-associated detergent molecules provide binding sites we may write

$$B = n(l_o + d_L) \quad \text{or} \quad n = B / (l_o + d_L)$$

where  $l_o$ ,  $d_L$  and  $n$  refer to the total lipid concentration, the concentration of detergent incorporated in the lipid phase and the number of  $\text{ANS}^-$  binding sites per amphiphile. The  $^{31}\text{P}$ -NMR measurements were performed on a WM 250 spectrometer (Bruker, Karlsruhe, F.R.G.) at a resonance frequency of 101.2 MHz. The magnetic field strength was stabilised with an internal  $^2\text{H}_2\text{O}$  lock. The flip angle of  $^{31}\text{P}$ -NMR pulses was  $90^\circ$  and the delay between Fourier pulses 3 s.

Areas under the inner and outer phosphate peaks of small unilamellar vesicles were measured after addition of 50  $\mu\text{l}$  of a 0.1 M  $\text{PrCl}_3$  solution to 1 ml of the vesicle/tensid dispersion. Average vesicle diameters were calculated assuming a bilayer thickness of 5 nm.

## Results

If carboxyfluorescein-filled liposomes (SUVs) are titrated with neutral detergents a steep increase in the efflux is observed at about one-fourth of the CMC (Fig. 1). At this point the morphological integrity of mixed bilayer liposomes is still preserved.

The changes in turbidity upon stepwise addition of OG and Triton X-100 to liposomes are shown in Fig. 2. A substantial turbidity increase was observed before solubilisation into mixed micelles. The effective detergent to lipid ratios at the point of maximal turbidity  $R_e(\text{OG}) = 0.81$  and  $R_e(\text{Triton X-100}) = 1.13$  are in reasonable agreement with the theoretical values (cf. Appendix).

Tensid-free SUVs had an average diameter of 26 nm as determined by  $^{31}\text{P}$ -NMR. Diameters increased already at quite low lipid to tensid ratios: 39 nm at  $R_e(\text{Triton X-100}) = 0.10$ , 31 nm at  $R_e(\text{OG}) = 0.11$  and 39 nm at  $R_e(\text{OG}) = 0.26$ .

The incorporation of the detergents into the lipid bilayer (sublytic range) decreases the phase transition temperature of DPPC liposomes progressively (Fig. 3).

The fluorescence intensity decays of DPH turned out to be biexponential in all cases studied as checked by the usual criteria of goodness of fit ( $\chi^2$ , Durbin-Watson test statistics, plot of residuals versus time and autocorrelation function of residuals). The values of the shorter lifetime  $\tau_2$  and its weighing factor  $a_2$  remained

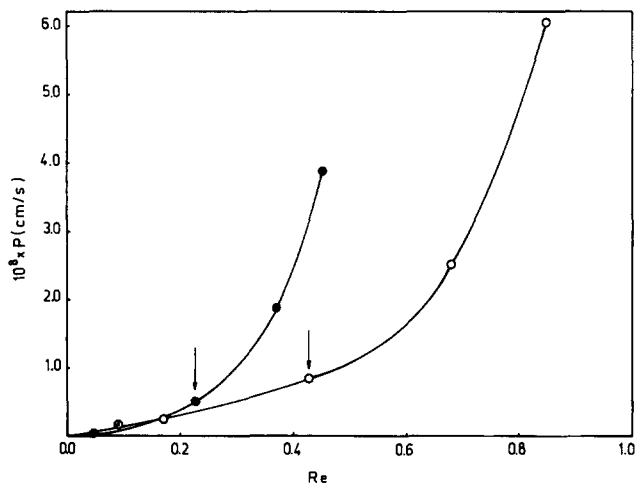


Fig. 1. Dependence of the permeability coefficient  $P$  (cm/s) of liposomally entrapped CF on the effective detergent to lipid ratio  $R_e = d_o / (l_o + 1/P\gamma)$  (cf. Appendix). ●—●, OG and ○—○, Triton X-100. Liposomes, REV(EPC), were shaped sequentially through 0.4 and 0.2  $\mu\text{m}$  polycarbonate filters (Nuclepore). Lipid concentration in the cuvette, 8.75  $\mu\text{M}$ ,  $T = 20^\circ\text{C}$ . The arrows indicate the point where the total detergent concentration has reached 1/4 CMC. The apparent vesicle diameter, evaluated as detailed in Methods, was 115 nm, from which a ratio volume/vesicle: membrane area/vesicle of  $6.4 \cdot 10^{-16} \text{ cm}^3$ :  $4.2 \cdot 10^{-10} \text{ cm}^2 = 1.5 \cdot 10^{-6} \text{ cm}$  was obtained.

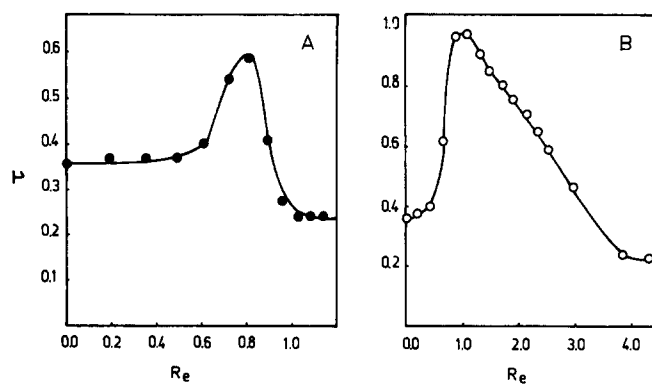


Fig. 2. Turbidity of EPC liposomes (SUVs) at various effective OG (panel A) and Triton X-100 (panel B) to lipid ratios  $R_e$  (cf. Eqn. A-7 of the Appendix,  $P(\text{OG}) = 58$  and  $P(\text{Triton X-100}) = 10000$ ). The turbidity, measured against buffer, was recorded after addition of detergent until a constant value was obtained (usually within a few minutes);  $T = 20^\circ\text{C}$ ; lipid concentrations  $< 3$  mM.

approximately constant ( $\tau_2 = 0.7 \pm 0.4$  ns and  $a_2 = 0.5 \pm 0.1$ ) independent of the composition of the sample. Thus, the behavior of the mean lifetime  $\langle \tau \rangle$  reflects mainly changes of the long-lived component  $\tau_1$  (see Table I). The mean lifetime increases slightly from 7.3 ns in pure EPC vesicles to values of about 8 ns after addition of OG (stage II). No significant lifetime changes were found in EPC/Triton X-100 mixed vesicles. Lifetimes in the range 7 to 8 ns are typical of this fluorophore in liquid-crystalline membranes [28]. Additional lifetime measurements of DPH in solvents of differing polarity yielded 8.3 ns in cyclohexane and 5.4 ns in methanol in agreement with conclusions reached by Parasassi et al. [28]. The findings above seem to suggest the hypothesis that OG reduces the polarity of the probe environment by a pronounced screening of the membrane interior from the water phase and/or translocation of the probe into deeper regions of the bilayer.

The steady-state anisotropy of DPH is rather low in EPC vesicles ( $r = 0.141$ ) and behaves quite differently when the vesicles are titrated with either OG or Triton

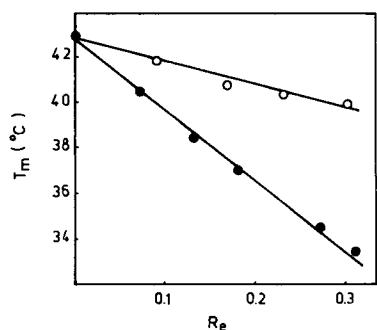


Fig. 3. Decrease of the phase transition temperature of DPPC vesicles after addition of OG or Triton X-100 in the sublytic range (stage I),  $R_e < R_e^c$ .  $R_e^c$ , the critical effective detergent to lipid ratio [3] is defined in Eqn. A-9 of the Appendix. Lipid concentration in the OG experiment, 0.66 mM, in the Triton X-100 experiment, 0.49 mM.

●—●, OG; ○—○, Triton X-100.

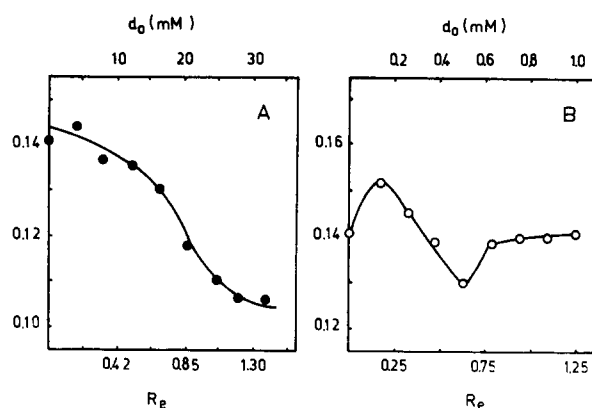


Fig. 4. Steady-state fluorescence anisotropy  $r$  of DPH incorporated in EPC vesicles. Anisotropy changes upon addition of OG (panel A) or Triton X-100 (panel B),  $l_o = 0.64$  mM. Marker to lipid ratio 1:200 (in A) and 1:300 (in B);  $\lambda_{\text{ex}}, 360$  nm;  $\lambda_{\text{em}}, 430$  nm.

X-100 (Fig. 4). The mean fluorescence lifetime of DPH in the pure lipid bilayer was 7.5 ns which might be compared with the value of 8.3 ns in cyclohexane. With Triton X-100 the mean lifetime in stage III (mixed micelles) amounted to 7.0 ns, nearly the same as in pure lipid (7.3 ns).

As steady-state measurements cannot answer the question whether the observed decrease in DPH anisotropy upon addition of OG is due to an increase in lifetime or a decrease in order the studies were extended to time-resolved anisotropy measurements. The results are assembled in Table I. It can be seen that the parameters which are sensitive to structural order of the bilayer ( $r_\infty$ ,  $S_{\text{DPH}}$  and  $r$ ) as well as the quantities reflecting lipid dynamics ( $\phi$ ,  $D_w$ ) show mostly only moderate changes which are, however, again quite different for OG and Triton X-100.

The steady-state anisotropy decreases monotonically with OG addition (cf. Fig. 4, A). On the other hand, it increases at low Triton X-100 concentrations ( $R_e < 0.2$ ), then decreases and, eventually, reverts to the initially value (cf. Fig. 4, B).

The lipid order parameter  $S_{\text{DPH}}$  decreases as Triton X-100 is incorporated in the bilayer as expected but increases again near the region of solubilisation. It behaves rather irregularly in the case of OG.

It was shown by Jähnig [23] by comparison with deuterium magnetic resonance ( $^2\text{H-NMR}$ ) data that  $S_{\text{DPH}}$  corresponds to the  $^2\text{H-NMR}$  order parameter of the acyl chain segment comprising carbons 10–12 suggesting that this may be the average location of the DPH molecule.

Both tensidors bring about a decrease in  $r_\infty$  and  $S_{\text{DPH}}$  indicating a lower degree of packing of the lipid fatty acid chains in mixed bilayers. At an effective detergent to lipid ratio less than 0.5 OG lowers the order parameter to a greater extent than Triton X-100. The most important and striking difference between the two de-

TABLE I

Parameters of total emission and anisotropy decays of DPH in EPC liposomes and in mixed OG/lipid and Triton X-100/lipid bilayers at 25°C

Lipid concentration  $l_0$ , 0.96 mM;  $r_\infty$ , limiting anisotropy;  $S_{\text{DPH}}$ , order parameter;  $\phi$ , relaxation time;  $D_w$ , wobbling diffusion constant;  $\langle\tau\rangle$ , average lifetime;  $\tau_1$ , lifetime of the long-lived component of the fluorescence decay. Standard deviations are on the average 10%, but less for fluorescence lifetime.

$R_e$	$r_\infty$	$S_{\text{DPH}}$	$\phi$ (ns)	$10^2 D_w$ ( $\text{ns}^{-1}$ )	$\langle\tau\rangle$ (ns)	$\tau_1$ (ns)
Pure EPC						
0.00	0.086	0.54	2.2	7.7	7.3	7.9
Triton X-100						
0.20	0.097	0.53	1.9	9.1	7.4	7.9
0.58	0.077	0.47	1.8	10.4	7.3	7.7
0.97	0.058	0.41	2.4	8.5	7.7	8.0
1.17	0.043	0.36	2.5	7.4	7.1	7.5
1.56	0.071	0.47	2.3	8.2	7.1	7.6
Octyl glucoside						
0.09	0.057	0.42	3.1	6.5	7.5	8.2
0.37	0.046	0.37	3.1	7.0	8.0	8.9
0.75	0.065	0.45	2.4	8.1	8.2	8.6
0.94	0.081	0.50	1.1	15.0	7.9	8.6
1.12	0.064	0.43	1.2	17.0	7.3	8.0
1.50	0.063	0.40	0.7	29.0	7.7	8.3

tergents is the much higher value of the wobbling diffusion constant  $D_w$  for OG as compared to Triton X-100 at  $R_e > 0.75$ .

An example of the binding isotherms for  $\text{ANS}^-$  obtained at increasing Triton X-100 concentrations is depicted in Fig. 5.

Further evaluation of the binding curves yielded the binding constants and the number of amphiphiles per  $\text{ANS}^-$  binding site (Figs. 6 and 7).

The binding capacity in pure lipid vesicles was found to be 12–13 phosphatidylcholines per  $\text{ANS}^-$  binding

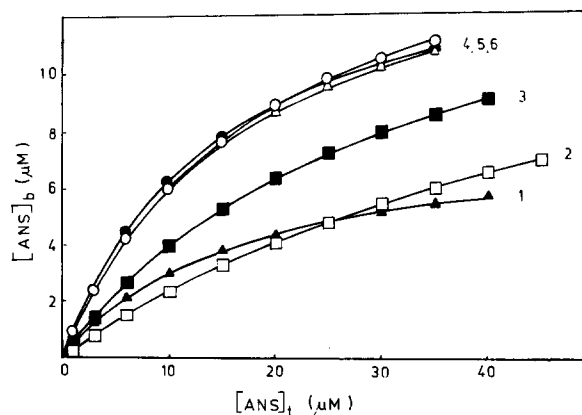


Fig. 5.  $\text{ANS}^-$  binding isotherms at various total Triton X-100 concentrations. 1, pure lipid, 0.1 mM (EPC liposomes); 2, pure detergent micelles;  $d_0 = 0.062$  mM (3), 0.125 mM (4), 0.188 mM (5) and 0.250 mM (6);  $d_0$  denotes the total detergent concentration.

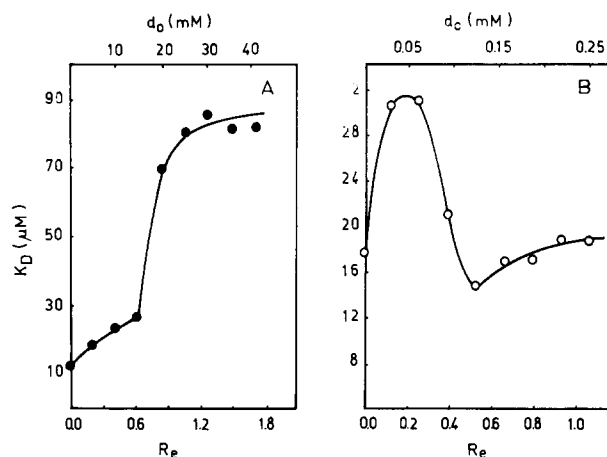


Fig. 6. Binding of  $\text{ANS}^-$  to EPC vesicles. The effect of varying ratios of detergent to lipid on the dissociation constant  $K_D$  of  $\text{ANS}^-$ . Panel A, OG; panel B, Triton X-100;  $l_0 = 0.1$  mM.

site. It decreases gradually to 3.5 in the OG experiment whereas Triton X-100 initially diminishes it to 8, then increases it up to 20. With OG there is a striking similarity between the course of the steady-state anisotropy of DPH (Fig. 4A) and the  $\text{ANS}^-$  binding capacity (Fig. 7A). As stated above,  $\text{ANS}^-$  binding is influenced by electrostatic interactions at the vesicle surface. The observed number of 12–13 phosphatidylcholine molecules per  $\text{ANS}^-$  binding site in pure lipid vesicles is higher than the four molecules reported at 1.5 M KCl [24]. An attempt was therefore made to work at 1 M KCl but technical reasons (aggregation of mixed bilayers and mixed micelles) precluded further experiments at this ionic strength. We note that here our interest is in surfactant-induced changes rather than in absolute values.

Vesicle affinities ( $1/K_D$ ) for  $\text{ANS}^-$  change similar to the binding capacity in the case of OG but with a jump

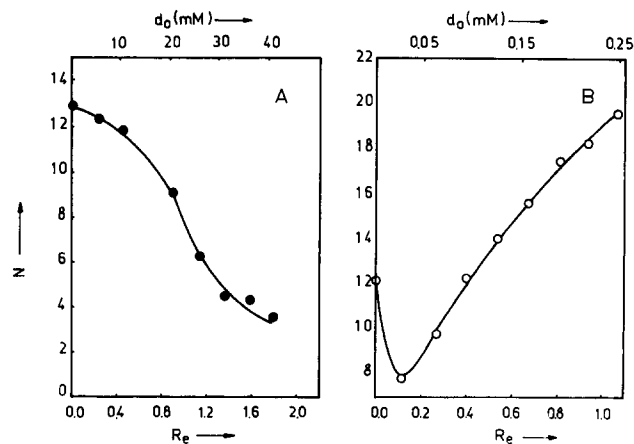


Fig. 7. Number of amphiphiles per  $\text{ANS}^-$  binding site ( $N$ ) as a function of the effective detergent to lipid ratio  $R_e$ . Lipid concentration  $l_0 = 0.1$  mM. Panel A, OG; panel B, Triton X-100.

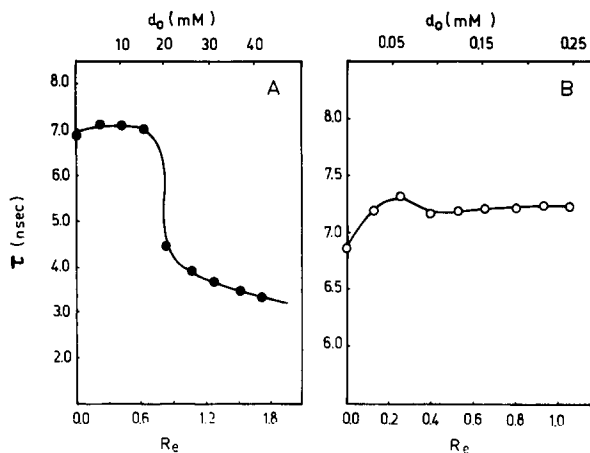


Fig. 8.  $\text{ANS}^-$  fluorescence lifetimes in pure EPC and mixed bilayer vesicles. Panel A, OG; panel B, Triton X-100;  $l_0 = 0.1$  mM.

in stage II and exhibit an initially biphasic behaviour in the Triton X-100 experiment.

$\text{ANS}^-$  fluorescence lifetimes (Fig. 8) change little in the sublytic range but jump to lower values in stage II of OG solubilisation.

## Discussion

To make meaningful and comparable measurements of changes of lipid membrane properties upon addition of detergents it is mandatory to correlate observed quantities with the actual (effective) detergent to lipid ratio within the membrane. A number of techniques has been adapted to the measurements of detergent 'binding' to lipid vesicles, such as gel filtration [4], ultracentrifugation [12], hygroscopic desorption [29] and rapid glass fiber filter filtration [4]. We use the bubble pressure method developed earlier [5] to estimate partition coefficients of detergents between the aqueous and lipid phase in liposomal dispersions. Detergents studied so far by this technique showed either constant or increasing partition coefficients when the surfactant concentration was raised in preformed SUV (EPC) suspensions (publication in preparation). In no case were saturation or decreasing partition coefficients observed. This seems to rule out binding into pre-existing sites and favours the equilibrium partition model (cf. Appendix). The partition coefficients are then used to calculate the effective detergent to lipid ratio  $R_e$  (cf. Eqn. (A-7), Appendix).

In this study we made an attempt to relate all observed membrane properties to  $R_e$  values. A word of caution is, however, in place. At present, some partition coefficients are likely to be inaccurate (e.g., Triton X-100) while others are highly reproducible (e.g., octyl glucoside). In addition, partition coefficients may vary considerably with the total surfactant to lipid ratio.

A very sensitive measure of the perturbation of membrane architecture by surfactants is the permeation of entrapped solutes. Our results (Fig. 1) confirm previous observations [30,31] of increases in membrane permeability below the critical micellar concentration (stage I). Carboxyfluorescein permeabilities of pure REV(EPC) liposomes were found to be around  $1 \cdot 10^{-9}$  (cm/s). They started to increase steeply at  $R_e = 0.23$  (OG) and  $R_e = 0.42$  (Triton X-100). At this point both detergents have reached but 1/4 of their CMC. A striking difference between B-type detergents (cholate, deoxycholate) and A-type detergents (OG, Triton X-100) was observed. Whereas the former released only a fraction of entrapped CF depending on the amount of surfactant added even after prolonged times (data not shown) thus corroborating the model of Schubert et al. [32] of formation of transient holes (discontinuous diffusion) the latter induced always a continuous solute liberation going to completion. This result is at variance with findings of Ruiz et al. [30] who report time-independent  $R_{50}$  values (total phospholipid to surfactant ratio producing 50% release of CF) for both types of surfactants. The reason for this discrepancy remains to be established.

Turbidity has been widely used to monitor membrane solubilisation. As increasing amounts of OG or Triton X-100 were added to preformed vesicles, the turbidity initially increases, passes through a maximum at an effective detergent to lipid ratio of about unit, and then decreases to a minimal value which reflects the turbidity of mixed micelles (Fig. 2). This phenomenon, also observed by others [11], indicates surfactant-induced aggregation, semifusion and fusion. Remarkably, the maximal Triton-induced turbidity could be reversibly reduced by agitation whereas the maximal OG-induced turbidity remained unchanged. This indicates, that aggregation and flocculation corresponding to the first and second minimum of the liposome interaction energy profile are less important in the latter case, i.e., fusion prevails. This is also corroborated by electron microscopy.

If we look at the results obtained with the fluorescent probes DPH and  $\text{ANS}^-$  (Figs. 4, 6–8, Table I), the following picture emerges: (i) there is a striking difference between the effects of octyl glucoside and Triton; (ii) increasing amounts of OG bring about a monotonic variation of most parameters which resembles a titration curve with a pronounced change around the critical effective detergent to lipid ratio; (iii) with Triton the behaviour is biphasic at very low  $R_e$  values and changes but little or not at all around the critical  $R_e$ .

What do these changes report? As judged from the changes of DPH fluorescence anisotropy ( $r$ ,  $\phi$ ,  $D_w$ ),  $\text{ANS}^-$  binding and  $T_m$  shifts, octyl glucoside perturbs the bilayer architecture in stage I to a greater extent than Triton, though the absolute changes are small. This

is true of the hydrophobic core as well as of the headgroup region.

The most pronounced effect is the increase in mobility of DPH with increasing OG concentration (Table I). After a steep transition in stage II the marker ends up with a higher mobility in OG/lipid mixed micelles. The decreasing ANS<sup>-</sup> fluorescence lifetime and binding affinity can be ascribed to an increasing exposition of the probe to water.

Evidently, as revealed by time-resolved anisotropy measurements, the OG-induced changes of the steady state anisotropy of DPH (Fig. 4A) are dominated by the kinetic component (fast relaxation) whereas the static component (static order,  $S_{\text{DPH}}$ ) does not change significantly.

The effect of Triton is different from that OG in several ways: (i) it seems to perturb the bilayer to a lesser extent (Figs. 1, 3B, 4B), (ii) ANS<sup>-</sup> in Triton/lipid mixed micelles, in contrast to the situation in OG/lipid micelles, is exposed to water to the same degree as in vesicles (Fig. 8) and (iii) neither the affinity towards ANS<sup>-</sup> (Fig. 6B) nor DPH mobility (Table I), nor static order (Table I) differ significantly from those in pure vesicles. We conclude that Triton/lipid micelles resemble vesicles with respect to structural order and mobility.

We interpret the changes seen at very low Triton concentrations ( $R_e < 0.2$ ) tentatively as packing optimisation in small unilamellar vesicles with high bilayer curvature by the wedge-shaped surfactant molecules as shown schematically in Fig. 9. In preliminary studies we found a decreased calcein efflux from sonicated EPC liposomes at a Triton to lipid ratio of  $R_e = 0.1$  (data not shown). Madden and Cullis [33] reported a stabilisation of unsaturated phosphatidylethanolamine bilayers by detergents which might be of relevance to our finding. Israelachvili et al. [34] analysed in detail how the change in packing of lipid molecules in the outer vesicle layer which takes place below a critical radius  $R_c$  leads to an increase of the hydrocarbon/water interface. The criti-

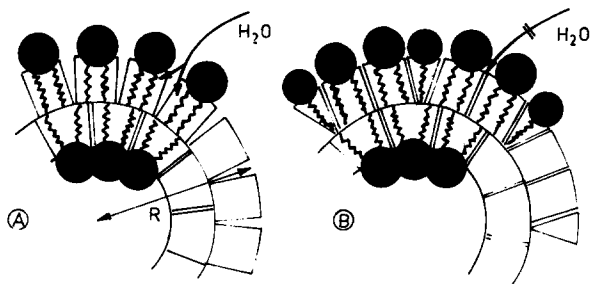


Fig. 9. Schematic representation of the packing of lipid molecules in small unilamellar vesicles (large bilayer curvature) illustrating the difference in the surface area available to polar headgroups in the inner and outer leaflet (A). Incorporation of wedge-shaped surfactant molecules improves packing in the outer layer making it less accessible to water (B). Headgroups are deliberately overdrawn.

cal radius of EPC vesicles, calculated from relation (7.11) of [34], is 10.4 nm. It must be kept in mind, however, that Israelachvili's self assembly theory of amphiphiles is based on an equilibrium size distribution whereas sonicated liposomes represent a metastable vesicle population. Taking this into account, Tenchov et al. [35] found a lower limit of the vesicle radius of 6 nm by fitting a Weibull distribution to vesicle size histograms. Vesicle size histograms of freeze-fracture micrographs of our preparations revealed numerous vesicles of lower size than those with  $R_c = 10.4$  nm. At least for this part of the vesicle population intercalation of Triton molecules into the outer leaflet would decrease the hydrocarbon/water interface.

Summarising the results, we conclude, that one cannot generalise the action of nonionic detergents on lipid bilayers. Rather, it depends on the molecular geometry, fraction and position of hydrophilic and lipophilic parts of the molecule. The interesting phenomenon of packing optimisation in small sonicated vesicles by suitable surfactants needs further experimentation.

## Appendix

### Equilibrium partition model

Starting with Nernst's equilibrium partition relation,  $P = d_1/d_w$ , we derived in 1983 [5] a partition equation which explicitly takes into account the volume fraction of lipid,  $V_1/V_o$ .

Here and further on, letters d and l denote detergent and lipid concentrations, respectively. Subscripts l and w refer to the lipid and aqueous phase (buffer), o to the total volume.  $P$  is the partition coefficient expressed in moles detergent in the lipid phase/lipid volume divided by moles of detergent in the aqueous phase/buffer volume. Briefly, the mass balance equation of detergent

$$d_o V_o = d_w V_w + d_l V_l$$

is recast\* into

$$d_o = d_w + d_l (V_l/V_o) \quad (\text{A-1})$$

assuming  $V_l < V_o$ , thus  $V_w \approx V_o$ .

The volume fraction of lipid,  $V_l/V_o$ , is then replaced by the total lipid concentration  $l_o$  times the molar volume of lipid  $\gamma^*$  yielding

$$d_l = (d_o - d_w)/\gamma l_o \quad (\text{A-2})$$

Hence

$$P = d_l/d_w = (d_o - d_w)/d_w \gamma l_o \quad (\text{A-3})$$

\* An estimate of  $\gamma$  can be obtained from the mean molecular volume of EPC or the partial specific volume times molecular weight of lipid:  $\gamma = 0.753$  (litre/mol) [5].

or

$$\gamma P = K = (d_o - d_w)/d_w l_o \quad (\text{A-4})$$

$K$  with the dimension of a binding constant may be viewed as a partition coefficient taking into account the volume ratio  $V_l/V_o$ , \*. If Eqn. A-3 is solved for  $d_w$  as measurable quantity,

$$d_w = d_o/(1 + P\gamma l_o) = m_o/(V_w + PV_l) \quad (\text{A-5})$$

where  $m_o$  is the total amount of detergent added, it becomes identical to that given by Lieb et al. [36] for the partitioning of anaesthetics into lipid bilayers.

As expected, Eqn. 5 predicts a linear relationship between the amount of detergent added and its equilibrium concentration in the aqueous phase and, consequently, in the lipid phase ( $d_l = Pd_o/(1 + P\gamma l_o)$ ). Though the equations above were derived under the assumptions  $d_o < l_o$  and  $d_o < \text{CMC}$ , experimental results [5,37] are surprisingly consistent with the equilibrium partition approach over a wide range of sublytic detergent concentrations.

Assuming that solubilisation occurs if the concentration of monomeric detergent in the aqueous phase reaches the CMC [3], that is  $d_w = \text{CMC}$ , we obtain from  $d_l = Pd_w$ , the critical detergent concentration in the lipid phase,  $d_l^c = P \cdot \text{CMC}$ . The critical total detergent concentration which, by definition, brings about solubilisation is then (cf. Eqn. A-1)

$$d_o^c = \text{CMC} + d_l^c (V_l/V_o)$$

$$d_o^c = \text{CMC} + P \cdot \text{CMC} \cdot \gamma \cdot l_o$$

$$d_o^c = \text{CMC}(1 + P\gamma l_o) \quad (\text{A-6})$$

Total detergent concentrations below this value are sublytic. The effective detergent to lipid ratio,  $R_e$ , introduced by Lichtenberg [3], is, by definition, simply

$$R_e = d_o(d_l V_l / (d_w V_w + d_l V_l)) / l_o$$

where the numerator represents the fraction of detergent in the lipid phase. Substituting again  $V_l/V_w \approx V_l/V_o = \gamma l_o$  and  $d_l/d_w = P$  leaves us with

$$R_e = d_o / (l_o + 1/P\gamma) \quad (\text{A-7})$$

The critical effective ratio is then

$$R_e^c = d_o^c / (l_o + 1/P\gamma) \quad (\text{A-8})$$

\* To avoid confusion, we point out that we and others [14,36] use moles detergent/respective volume (lipid and water volume) whereas Lichtenberg [3] gives all detergent concentrations per unit total volume.

Combining Eqns. A6 and A-8

$$R_e^c (l_o + 1/P\gamma) = \text{CMC}(1 + P\gamma l_o)$$

reveals by comparison of the left and right hand side that

$$R_e^c = P \cdot \gamma \cdot \text{CMC} \quad (\text{A-9})$$

For the detergents studied we obtain with  $P(\text{OG}) = 58$  [5] and  $P(\text{Triton X-100}) = 10\,000$  [4],  $R_e^c(\text{OG}) = 58 \cdot 0.753 \cdot 0.021 = 0.92$  and  $R_e^c(\text{Triton X-100}) = 10\,000 \cdot 0.753 \cdot 0.00024 = 1.81$ .

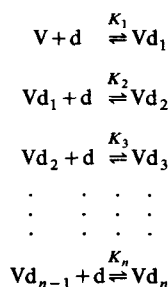
$R_e$  and  $R_e^c$  values for Triton X-100 are likely to be much more uncertain than those for OG because it is notoriously difficult to measure true equilibrium partition coefficients with this type of detergent as, depending on the procedure employed, metastable mixtures are obtained. In the literature,  $P(\text{Triton X-100})$  values vary between 660 [12] and 400 000 [38].

More consistent values are reported for the similar but homogeneous detergent octaethyleneglycol dodecyl monoether ( $\text{C}_{12}\text{O}_8$ ), 7570 [3] and 10 000 [4].

In the partition model the coefficient  $P$  can be assumed to be independent of the degree of advancement of the 'reaction' when the solubility of the surfactant in one or the other phase is not exceeded.

#### Binding model

Let us assume that one lipid vesicle has  $n$  binding sites for detergent molecules resulting in the following multiple binding equilibria



The binding function is then given by:

$r$  = moles of detergent bound / moles of vesicles, hence  $r = m_b / (\text{moles lipid} / \text{number of lipid molecules per vesicle})$ . In order to express  $r$  in terms of binding constants and free detergent concentration we proceed in the same way as in the treatment of multiple binding of ligands to proteins [39] and obtain, assuming all intrinsic binding constants to be equal and independent, that is  $K_i = ((n + i + 1)/i) \cdot K$ ,

$$r' = n' K d_w / (1 + K d_w) \quad (\text{A-10})$$

where  $n'$  is the number of binding sites per molecule of

lipid and  $r'$  = moles of detergent/mole of lipid. Eqn. A-10 can be rewritten as

$$(m_b/V_o) \cdot (V_o/V_1) = (n'l_o Kd_w / (1 + Kd_w)) \cdot (V_o/V_1)$$

$$d_1 = n'Kd_w / \gamma(1 + Kd_w) \quad (\text{A-11})$$

which is the equation of a binding isotherm. If the  $K_i$  values were not equal (i.e., heterogeneity of binding sites), we would obtain an Adair type of binding equation which can model positive (sigmoidal binding curve) or negative cooperativity of detergent binding.

Recasting Eqn. A-11 into

$$P = d_1/d_w = n'K/\gamma(1 + Kd_w) \quad (\text{A-12})$$

it is seen that, if binding would be the adequate description of detergent liposome interactions,  $P$  should be a monotonously decreasing function of the free detergent concentration  $d_w$ .

## References

- 1 Helenius, A. and Simons, K. (1975) *Biochim. Biophys. Acta* 415, 29–79.
- 2 Ueno, M., Tanford, Ch. and Reynolds, J.A. (1984) *Biochemistry* 23, 3070–3076.
- 3 Lichtenberg, D. (1985) *Biochim. Biophys. Acta* 821, 470–478.
- 4 Le Maire, M., Moller, J.V. and Champeil, P. (1987) *Biochemistry* 26, 4803–4810.
- 5 Lasch, J., Berdichevsky, V.R., Torchilin, V.P., Koelsch, R. and Kretschmer, K. (1983) *Anal. Biochem.* 133, 486–491.
- 6 Moller, J.V., Le Maire, M. and Andersen, J.P. (1986) in *Progress in Protein-Lipid Interactions* (Watts, A. and De Pont, J.J.H.H.M., eds.), Vol. 2, pp. 147–196, Elsevier Science Publishers, Amsterdam.
- 7 Racker, E. (1979) *Methods Enzymol.* 55, 699–711.
- 8 Eytan, G.D. (1982) *Biochim. Biophys. Acta* 694, 185–202.
- 9 Zumbühl, O. and Wender, H.G. (1981) *Biochim. Biophys. Acta* 640, 252b1262.
- 10 Schurtenberger, P., Mazer, N. and Waldvogel, S. (1984) *Biochim. Biophys. Acta* 775, 111–114.
- 11 Jackson, M.L., Schmidt, C.F., Lichtenberg, D., Litman, B.J. and Albert, A.D. (1982) *Biochemistry* 21, 4576–4582.
- 12 Goni, F.M., Urbaneja, M.-A., Arrondo, J.L.R., Alonso, A. and Durrani, A.A. (1986) *Eur. J. Biochem.* 160, 659–665.
- 13 Bayerl, T., Klose, G., Blanck, J. and Ruckpaul, K. (1986) *Biochim. Biophys. Acta* 858, 285–293.
- 14 Van Dael, H. and Ceuterickx, P. (1984) *Chem. Phys. Lipids* 35, 171–181.
- 15 Szoka, F., Olson, F., Heath, T., Vail, W., Mayhew, E. and Papa-hadjopoulos, D. (1980) *Biochim. Biophys. Acta* 601, 559–571.
- 16 Stewart, J.Ch.M. (1980) *Anal. Biochem.* 104, 10–14.
- 17 Weinstein, T.N., Yoshikami, S., Heukart, P., Blumenthal, R. and Hagins, W.A. (1977) *Science* 195, 489–491.
- 18 Mimms, L.T., Zampighi, G., Nozaki, Y., Tanford, Ch. and Reynolds, J.A. (1981) *Biochemistry* 20, 833–840.
- 19 Gaub, H., Büschl, R. and Ringsdorf, H. (1985) *Chem. Phys. Lipids* 35, 19–43.
- 20 Dale, R.E., Chen, L.A. and Brand, L. (1977) *J. Biol. Chem.* 252, 7500–7540.
- 21 Ameloot, M., Hendrickx, H., Herreman, W., Pottel, H., Van Cauwelaert, F. and Van der Meer, W. (1984) *Biophys. J.* 46, 525–539.
- 22 Kinoshita, K., Jr., Kawato, S. and Ikegami, A. (1977) *Biophys. J.* 30, 289–305.
- 23 Jähnig, F. (1979) *Proc. Natl. Acad. Sci. USA* 76, 6361–6365.
- 24 Blitterswijk, W.J., Van Hoeven, R.P. and Van der Meer, B.W. (1981) *Biochim. Biophys. Acta* 644, 323–332.
- 25 Lipari, G. and Szabo, A. (1980) *Biophys. J.* 30, 489–506.
- 26 Radda, G.K. and Vanderkooi, J. (1972) *Biochim. Biophys. Acta* 265, 509–549.
- 27 Haynes, D.H. and Staerk, H. (1974) *J. Membr. Biol.* 17, 313–340.
- 28 Parasassi, T., Conti, F., Glaser, M. and Gratton, E. (1984) *J. Biol. Chem.* 259, 14011–14017.
- 29 Conrad, M.J. and Singer, S.J. (1981) *Biochemistry* 20, 808–818.
- 30 Ruiz, J., Goni, F.M. and Alonso, A. (1988) *Biochim. Biophys. Acta* 937, 127–134.
- 31 O'Connor, C.J., Wallace, R.G., Iwamoto, K., Taguchi, T. and Sunamoto, J. (1985) *Biochim. Biophys. Acta* 817, 95–102.
- 32 Schubert, R., Beyer, K., Wollburg, H. and Schmidt, K.-H. (1986) *Biochemistry* 25, 5263–5269.
- 33 Madden, T.D. and Cullis, P.R. (1982) *Biochim. Biophys. Acta* 684, 149–153.
- 34 Israelachvili, J.N., Mitchell, D.J. and Ninham, B.W. (1976) *J. Chem. Soc.* 72, 1525–1568.
- 35 Tenchov, B.G., Yanev, T.K., Tihova, M.G. and Koynova, R.D. (1985) *Biochim. Biophys. Acta* 816, 122–130.
- 36 Lieb, W.R., Kovalycsik, M. and Mendelsohn, R. (1982) *Biochim. Biophys. Acta* 688, 388–398.
- 37 Schurtenberger, P., Mazer, N.A. and Kanzig, W. (1985) *J. Phys. Chem.* 89, 1042–1049.
- 38 Hoffmann, J. (1988) Thesis, Martin-Luther-University, Halle/Saale, G.D.R.
- 39 Hammes, G.G. (1982) *Enzyme Catalysis and Regulation*, pp. 161–162, Academic Press, New York.